Journal of Solid State Chemistry **165,** 89–93 (2002)
doi:10.1006/jssc.2001.9502, available online at http://www/idealibrary.com on IDEAL®

A Copper Uranyl Monophosphate Built Up from $[CuO_2]_\infty$ Chains: $Cu_2UO_2(PO_4)_2$

A. Guesdon,[1] J. Chardon, J. Provost, and B. Raveau

Laboratoire CRISMAT, UMR 6508 associée au CNRS, ISMRA, 6, Boulevard du Maréchal Juin, 14050 Caen Cedex, France

Received September 17, 2001; in revised form December 26, 2001; accepted January 4, 2002

A copper uranyl monophosphate, $Cu_2UO_2(PO_4)_2$, has been synthesized for the first time. It crystallizes in the space group $C2/m$ with $a = 14.040(1)$ Å, $b = 5.7595(4)$ Å, $c = 5.0278(5)$ Å and $\beta = 107.24(1)^\circ$. Its original structure consists of $[CuO_2]_\infty$ puckered chains of edge-sharing CuO_4 groups running along b, interconnected with $[UP_2O_{10}]_\infty$ ribbons. The coordination of uranium is characteristic of the $[UO_2]^{2+}$ uranyl ion, forming flattened UO_6 octahedra, whereas the planar CuO_4 groups exhibit a rectangular configuration. This compound shows original antiferromagnetic interactions at low temperature, due to the presence of $[CuO_2]_\infty$ chains, but the latter are more complex than those of 1-D spin $\frac{1}{2}$ chains. © 2002 Elsevier Science (USA)

INTRODUCTION

In the vast field of research on oxides, copper was revealed to be a very attractive element, as shown by the discovery of superconductive cuprates (for a review see Refs. 1–3), the important study on the spin Peierls transition in $CuGeO_3$ (4–6), and the recent investigation of the transparent conductor $CuAlO_2$ with the delafossite structure (7, 8). The introduction of copper into a phosphate matrix is also of great interest, but it requires the association of a second transition element or of an actinide. This is, for example, the case of the phosphates $CuZr_2(PO_4)$ and $CuTh_2(PO_4)_3$ (9), which exhibit interesting fluorescence properties (10, 11) and are also active catalysts (12).

Recent studies on uranyl phosphates, such as $U(UO_2)(PO_4)_2$ (13), $(NHEt_3)(UO_2)_2PO_4(HPO_4)$, $NPr_4(UO_2)_3(PO_4)(HPO_4)_2$ (14), and $Ba_3UO_2(PO_4)(PO_3OH)_2{\cdot}xH_2O$ (15), suggest the possibility of creating new mixed frameworks involving both copper and uranium in the same matrix. Such a hypothesis is corroborated by the existence of the mineral metatorbernite, $Cu(UO_2PO_4)_2{\cdot}8H_2O$ (16), which consists of uranyl phosphate layers interleaved with $[Cu(H_2O)_4]^{2+}$ cations. We have thus investigated the Cu–U–P–O system. In the present study we describe the original structure and magnetic properties of the first anhydrous uranyl phosphate, $Cu_2UO_2(PO_4)_2$, that has been synthesized to date.

[1]To whom correspondence should be addressed. E-mail: guesdon@ismra.fr. Fax: 33 2 31 95 16 00.

EXPERIMENTAL

Crystal Growth and EDS Analysis

The single crystal used for structure determination of the title compound was extracted from a mixture of nominal composition "$Cu_2U_2P_2O_{11}$" prepared in the following way: CuO, UO_2, and P_2O_5 were mixed in adequate ratios in a glove box under nitrogen atmosphere; the finely ground mixture was placed in an evacuated silica tube which was then sealed. It was heated at 1423 K for 50 h, cooled at 10°/h down to 923 K, and finally allowed to cool to room temperature in the furnace, the heater being shut off. The result was a mixture of several unidentified phases: a black powder containing red, green, and black crystals was obtained.

The EDS analysis, performed with an Oxford 6650 microprobe mounted on a Philips XL 30 FEG scanning electron microscope, evidenced the presence of Cu, U, and P in the green crystals, confirming the ratio 2:1:2.

Single-Crystal X-Ray Diffraction Study

Several green crystals were selected optically and tested by the oscillation and Weissenberg methods using Cu$K\alpha$ radiation. A single crystal with dimensions $0.077 \times 0.051 \times 0.038\,mm^3$ was thus chosen for the structure determination. The cell parameters given in Table 1 were determined and refined by diffractometric techniques at 293 K using a least-squares method based on 25 reflections in the range $18^\circ < \theta < 22^\circ$. The data were collected on a CAD4 Enraf–Nonius diffractometer using Mo$K\alpha$ radiation; the data collection parameters are reported in Table 1.

0022-4596/02 $35.00

TABLE 1
Crystal Data, Intensity Measurements, and Structure Refinement Parameters for $Cu_2^{II}U^{VI}O_2(PO_4)_2$

Crystal data	
Space group	$C2/m$ (No. 12)
Cell dimensions	$a = 14.040(1)$ Å
	$b = 5.7595(4)$ Å
	$c = 5.0278(5)$ Å
	$\beta = 107.24(1)^\circ$
Volume	388.3 Å^3
Z	2
ρ_{calc}	5.021 g cm^{-3}
Intensity measurements	
λ(Mo$K\alpha$)	0.71073
Scan mode	ω–θ
Scan width	$1.0 + 0.35 \tan\theta$
Slit aperture (mm)	$1.10 + \tan\theta$ mm
Max θ	45°
Standard reflections	3 measured every 3600 s
Measured reflections	3422
Reflections with $I > 3\sigma$ (I)	2703
Independent reflections with $I > 3\sigma(I)$	1420
μ	26.683 mm^{-1}
Structure solution and refinement	
Parameters refined	45
Agreement factors	$R(F) = 0.029$ $R_w(F) = 0.028$
Weighting scheme	$w = 1/\sigma^2$
Δ/σ max	$<10^{-4}$

TABLE 2
Positional Parameters and Their Estimated Standard Deviations in $Cu_2UO_2(PO_4)_2$

Atom	x	y	z	$U_{eq}*100$ (Å^2)
Cu	$\frac{1}{4}$	$\frac{1}{4}$	$\frac{1}{2}$	0.99(2)
U	0	0	0	0.62(1)
P	0.35015(8)	0	0.0813(2)	0.68(4)
O(1)	0.0909(3)	0	0.3354(8)	1.6(2)
O(2)	0.0879(2)	0.2820(4)	−0.1327(6)	1.5(1)
O(3)	0.2831(2)	0	0.2783(7)	0.9(1)
O(4)	$0.280_2(3)$	0	−0.2235(7)	1.1(1)

Note. All atoms were refined anisotropically and are given in the form of the isotropic equivalent displacement parameter U_{eq} defined as one-third of the trace of the orthogonalized U_{ij} tensor.

The reflections were corrected for Lorentz and polarization effects and for absorption and secondary extinction. The structure was solved in the centrosymmetric $C2/m$ space group (No. 12) with the heavy atom method and subsequent difference Fourier and Fourier series, leading to the formula $Cu_2UO_2(PO_4)_2$. Refinement of the atomic coordinates and of the anisotropic thermal factors of all atoms led to $R(F) = 0.029$ and $R_w(F) = 0.028$ and to the atomic parameters listed in Table 2. The calculations were performed with the Xtal 3.7 program (17).

Chemical Synthesis, Powder X-Ray Diffraction Study, and Magnetic Measurements

Synthesis of this new uranium(VI) monophosphate $Cu_2UO_2(PO_4)_2$ as a pure powder sample was performed in three steps: first, an intimate mixture of $Cu(NO_3)_2 \cdot 3H_2O$, $(NO_3)_2UO_2 \cdot 6H_2O$, and $(NH_4)_2HPO_4$ (molar ratios 2:1:2) was heated in a platinum crucible in air at 673 K to decompose the nitrates and the ammonium phosphate. Once the correct weight loss was achieved, the mixture was finely ground and heated in air in a covered alumina crucible at 1273 K for 12 h; it was then ground again and finally heated at 1323 K for 12 h, leading to a green powder. Its X-ray diffraction pattern was collected with a Philips PW 1830 diffractometer using Cu$K\alpha$ radiation in steps of 0.02° in 2θ within the angular range $5^\circ \leq 2\theta \leq 115^\circ$. It was indexed in a monoclinic cell in agreement with that obtained from the single-crystal study. The refinement of the cell parameters, performed with the Fullprof program (18) in pattern matching mode, led indeed to $a = 14.0363(3)$, $b = 5.7605(1)$, $c = 5.0258(1)$, $\beta = 107.140(1)$, $V = 388.32(1)$ with the following agreement factors: $R_p = 5.92$, $R_{wp} = 7.59$, and $\chi^2 = 2.23$.

Magnetic susceptibility measurements were performed on a powder sample of $Cu_2UO_2(PO_4)_2$ by SQUID magnetometry. After zero field cooling and stabilization of the temperature at 4.5 K, a magnetic field of 0.3 T was applied. The magnetic moments were then measured with increasing temperature up to 300 K.

DESCRIPTION OF THE STRUCTURE AND DISCUSSION

The structure of $Cu_2UO_2(PO_4)_2$ is built from an assemblage of UO_6 octahedra with PO_4 tetrahedra and CuO_4 planar groups. Its projections along **a** (Fig. 1) and **c** (Fig. 2) axes show that this structure can easily be described from $[UP_2O_{10}]_\infty$ chains and $[CuO_2]_\infty$ ribbons of edge-sharing CuO_4 planar groups. One can indeed observe that each UO_6 octahedron shares its four equatorial apices with four monophosphate groups to form $[UP_2O_{10}]_\infty$ chains parallel to the [010] direction (Figs. 1 and 2). In such chains, which form square-shaped windows delimited by two octahedra and two tetrahedra (Fig. 2), each PO_4 group is linked to two UO_6 octahedra and shares its two remaining corners with two $[CuO_2]_\infty$ ribbons (Fig. 1). Reciprocally, each $[CuO_2]_\infty$ ribbon shares its oxygen atoms with the PO_4 tetrahedra of four different $[UP_2O_{10}]_\infty$ chains (Fig. 3). One remarkable feature of this structure concerns the geometry of the $[CuO_2]_\infty$ ribbons which are not planar, but are puckered, two successive CuO_4 groups forming an angle of 147.15° (Fig. 2) with Cu–Cu distances of 2.88 Å. Finally it is worth noting that, along the [100] direction, two successive $[UP_2O_{10}]_\infty$ chains (or two successive $[CuO_2]_\infty$ ribbons) are deduced one from

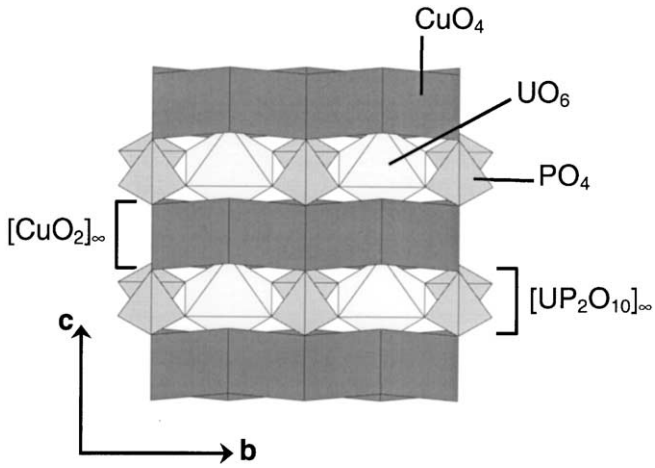

FIG. 1. Projection of the structure of $Cu_2UO_2(PO_4)_2$ along **a.**

the other through the $(\mathbf{a}+\mathbf{b})/2$ shift of the C lattice translation. The resulting three-dimensional framework presents pentagonal tunnels parallel to [001] (Fig. 2) and S-shaped tunnels running along **b** (Fig. 3).

The uranium atom is surrounded by six oxygen atoms forming a flattened octahedron (Table 3). There are indeed two kinds of U–O distances in this polyhedron: (i) two short apical U–O(1) bonds of 1.788(3) Å making an O(1) – U–O(1^i) angle of 180°, which corresponds to the characteristic geometry of the $[UO_2]^{2+}$ uranyl ion; (ii) four longer U–O(2) distances of 2.257(3) Å, approximately perpendicular to the previous ones and forming the equatorial plane of the UO_6 octahedron. This environment is in good agreement with that usually observed for U(VI) in a sixfold coordination, since the average value of the U–O bondlengths in these octahedra is 2.26(8) Å for the equatorial U–O distances and about 1.8 Å in the $(UO_2)^{2+}$ uranyl ion (19).

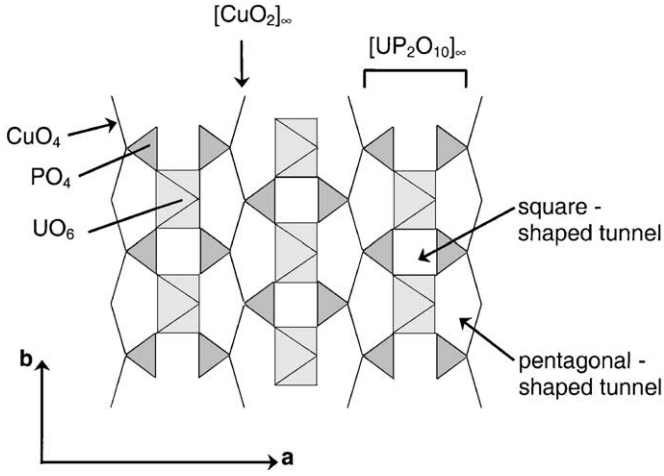

FIG. 2. Projection of the structure of $Cu_2UO_2(PO_4)_2$ along **c.**

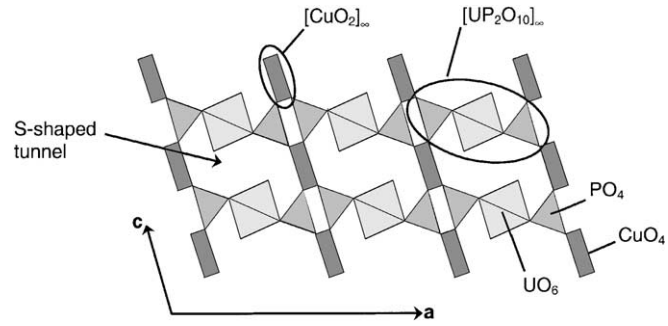

FIG. 3. Projection of the structure of $Cu_2UO_2(PO_4)_2$ along **b.**

The PO_4 tetrahedron presents two groups of P–O distances: one can indeed observes two P–O(2) bonds of 1.505(3) Å corresponding to the corners shared with two UO_6 octahedra, and two longer distances of 1.556 Å for the oxygen atoms shared with the $[CuO_2]_\infty$ ribbons. However, the tetrahedron is quite regular, since the O–O distances and the O–P–O angles are rather homogeneous, in agreement with the geometry usually observed for monophosphate groups (Table 3).

The copper atom is surrounded by four oxygen atoms sitting in a plane. However, although the four Cu–O distances are equal (1.959(3) Å), there are two O(3)–Cu–O(4) angles of 80° and two of 100°, so that the copper atom is in a rectangular environment with two sorts of O–O distances: 2.517 and 3.002 Å (Table 3). Note that this rectangular surrounding is not unusual for Cu^{2+} cations, especially when the CuO_4 groups share two of their edges to form $[CuO_2]_\infty$ ribbons. This is the case, for instance, in the copper oxides Cu_4O_3, $BaCuO_4$, and Li_2CuO_2 (20–22), in which the CuO_4 planes present two shortest O–O distances corresponding to the shared edges, whereas the two remaining O–O bonds are longest. However, the rectangular distortion is less accentuated in $BaCuO_4$ and Li_2CuO_2, with short O–O distances of about 2.65 Å and long O–O distances of about 2.85 Å, whereas their values are in the CuO_4 group of the paramelaconite Cu_3O_4 of 2.56 and 2.92 Å, respectively. Finally, one can note that, although the $[CuO_2]_\infty$ ribbons are flat in many structures involving CuO_4 groups joined through an edge, as for instance in the $(A_{1-x}A'_x)_{14}Cu_{24}O_{41}$ compounds (23, 24), the titled compound exhibits puckered ribbons similar to those of the paramelaconite Cu_4O_3 (20).

The divalent character of copper in $Cu_2UO_2(PO_4)_2$ has been confirmed by the valence calculations (25) which led to a value of 1.9.

Magnetic Susceptibility

Figure 4 gives the molar susceptibility versus temperature for $Cu_2UO_2(PO_4)_2$. For $T > 150$ K, the data were

TABLE 3
Distances (Å) and Angles (°) in $Cu_2UO_2(PO4)_2$

U	O(1)	O(1^{i})	O(2)	O(2^{i})	O(2^{ii})	O(2^{iii})
O(1)	1.788(3)	3.576(5)	2.850(5)	2.909(4)	2.850(5)	2.909(4)
O(1^{i})[a]	180.0	1.788(3)	2.909(4)	2.850(5)	2.909(4)	2.850(5)
O(2)	88.8(1)	91.2(1)	2.257(3)	4.515(4)	3.248(4)	3.135(4)
O(2^{i})	91.2(1)	88.8(1)	180.0	2.257(3)	3.135(4)	3.248(4)
O(2^{ii})	88.8(1)	91.2(1)	92.0(1)	88.0(1)	2.257(3)	4.515(4)
O(2^{iii})	91.2(1)	88.8(1)	88.0(1)	92.0(1)	180.0	2.257(3)
P	O(2iv)	O(2v)	O(3)	O(4)		
O(2^{iv})	1.505(3)	2.511(4)	2.485(4)	2.499(4)		
O(2^{v})	113.1(2)	1.505(3)	2.485(4)	2.499(4)		
O(3)	108.6(2)	108.6(2)	1.556(4)	2.511(5)		
O(4)	109.4(1)	109.4(1)	107.6(2)	1.556(3)		
Cu	O(3)	O(3^{vi})	O(4^{iv})	O(4^{vii})		
O(3)	1.959(3)	3.919(4)	3.002(1)	2.517(5)		
O(3^{vi})	180.0	1.959(3)	2.517(5)	3.002(1)		
O(4^{iv})	100.0(1)	80.0(1)	1.959(2)	3.919(4)		
O(4^{vii})	80.0(1)	100.0(1)	180.0	1.959(2)		

[a](i) $-x, -y, -z$; (ii) $x, -y, z$; (iii): $x, y, -z$; (iv) $\frac{1}{2}-x, \frac{1}{2}-y, -z$; (v) $\frac{1}{2}-x, -\frac{1}{2}+y, -z$; (vi) $-x, \frac{1}{2}-y, 1-z$; (vii) $x, y, 1+z$.

fitted with a Curie–Weiss law: $\chi_m = C/(T\text{-}\theta)$. The fitting parameter C led to a paramagnetic moment of $2.0\mu_B$ per Cu^{2+} ion, which is in agreement with the expected value. The χ_m(T) curve presents a broad maximum at around 50 K, characteristic of the transition toward an antiferromagnetic ordering in agreement with the θ fitting value : $\theta = -43$ K. Attempts to fit the (T) curve with models for one-dimensional spin $\frac{1}{2}$ chains failed. The best fit was obtained with the $S=\frac{1}{2}$ Heisenberg infinite chain model through the equation from (26), but with a fitting parameter $g = 3.37$, which is an unacceptable value. The fitting curve is very far from the experimental one if g at is set 2. Two other simple models were tested to fit the data, a dimer model (27) and the Ising model (28), but these tests were not successful. Further experimental and theoretical studies are necessary to try to understand the magnetic properties of this compound.

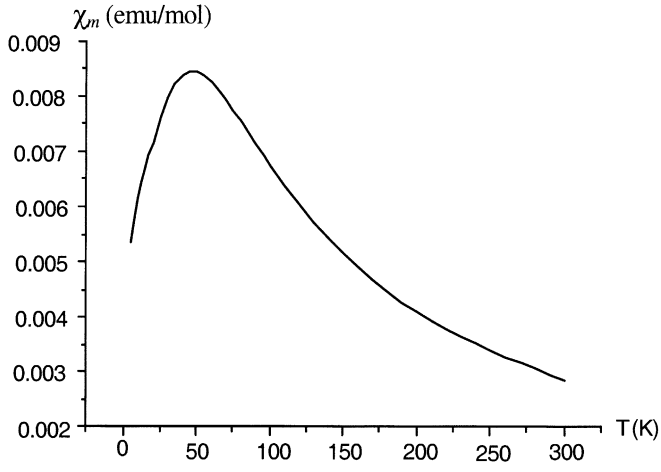

FIG. 4. Molar susceptibility versus temperature for $Cu_2UO_2(PO_4)_2$.

CONCLUSION

$Cu_2UO_2(PO_4)_2$ is the first anhydrous copper uranyl phosphate that has been synthesized to date. Its very simple structure, involving $[CuO_2]_\infty$ puckered chains, is of great interest for the study of the magnetic properties of unidimensionnal spin $\frac{1}{2}$ systems. Growth of larger crystals will be necessary to explore the magnetic behavior of this compound.

REFERENCES

1. B. L. Chamberland, *in* "Chemistry of Superconductors Materials" (T. A. Vanderah, Ed.), pp. 2– 105, Noyes, 1992.
2. B. Raveau, C. Michel, M. Hervieu, and D. Groult, "Crystal Chemistry of High T_c Superconducting Copper Oxides." Springer-Verlag, Berlin/NewYork 1991.
3. J. G. Bednorz and K. A. Müller (Eds.), "Earlier and Recent Aspects of Superconductivity," Springer Series in Solid State Sciences 90. Springer-Verlag, Berlin, 1990.
4. J. P. Renard, K. Le Dang, P. Veillet, G. Dhalenne, A. Revcolevschi, and L. P. Regnault, *Europhys. Lett.* **30,** 475 (1995).
5. K. Manabe, H. Ishimoto, N. Koide, Y. Sasago, and K. Uchinokura, *Phys. Rev. B* **58,** 575 (1998).
6. J. P. Boucher and L. P. Regnault, *J. Phys. I Fr.* **6,** 1939 (1996).
7. F. A. Benko and F. P. Koffyberg, *J. Phys. Chem. Solids* **45,** 57 (1984).

8. H. Kawazoe, M. Yasukawa, H. Hyodo, M. Kuita, H. Yanagi, and H. Hosono, *Nature* **389,** 939 (1997).
9. M. Loüer, R. Brochu, and D. Loüer, *Acta Crystallogr. Sect. B* **51,** 908 (1995).
10. W. F. Schmid and R. W. Mooney, *J. Electrochem. Soc.* **111,** 668 (1964).
11. G. Le Polles, C. Parent, A. Olazcuaga, G. Leflem, and P. Hagenmuller, *C.R. Acad. Sci.* **306,** 765 (1988).
12. A. Serghini, M. Kacimi, M. Ziyad, and R. Brochu, *J. Chim. Phys. Chim. Biol.* **85,** 449 (1988).
13. P. Bernard, D. Louër, N. Dacheux, V. Brandel, and M. Genet, *Chem. Mater.* **6,** 1049 (1994).
14. R. J. Francis, M. J. Drewitt, P. S. Halasyamani, C. Ranganathachar, D. O'Hare, W. Clegg, and S. J. Teat, *Chem. Commun.* **2,** 279 (1998).
15. A. Guesdon and B. Raveau, *Chem. Mater.* **10,** 3471 (1998).
16. N. J. Calos and C. H. Kennard, *Z. Kristallogr.* **211,** 701 (1996).
17. S. R. Hall, D. J. du Boulay, and R. Olthof-Hazekamp (Eds.), "Xtal 3.7 System." Univ. of Western Australia, 2000.
18. J. Rodriguez-Carjaval, *in* "Satellite Meeting on Powder Diffraction: Abstracts of the XVth Conference of the International Union of Crystallography, Toulouse" (J. Galy, Ed.), p. 127, 1990.
19. P. C. Burns, M. L. Miller, R. C. Ewing, *Can. Mineral.* **34,** 845 (1996).
20. M. O'Keefe and J. O. Bovin, *Am. Mineral.* **63,** 180 (1978).
21. R. Kipka, and Hk. Müller-Buschbaum, *Z. Naturforsch. B* **32,** 121 (1977).
22. R. Hoffmann, R. Hoppe, and W. Schaefer, *Z. Anorg. Allg. Chem.* **578,** 18 (1989).
23. T. Siegrist, L. F. Scheemeyer, S. A. Sunshine, J. V. Waszak, and R. S. Roth, *Mater. Res. Bull.* **23,** 1429 (1988).
24. E. M. Mac Carron, M. A. Subramanian, J. C. Calabrese, and R. L. Harlow, *Mater. Res. Bull.* **23,** 1355 (1988).
25. N. E. Brese and M. O'Keefe, *Acta. Crystallogr. Sect. B* **47,** 192 (1991).
26. W. E. Hatfield, *J. Appl. Phys.* **52,** 1985 (1981).
27. Bleaney-Bowers, F. E. Mabbs, and D. J. Martin, "Magnetism and Transition Metal Complexes," Chapman & Hall, London, 1974.
28. M. E. Fischer, *J. Mater. Phys.* **4,** 124 (1963).